ACS APPLIED MATERIALS & INTERFACES

Research Article

www.acsami.org

Phenotypic Modulation of Smooth Muscle Cells by Chemical and Mechanical Cues of Electrospun Tecophilic/Gelatin Nanofibers

Elham Vatankhah,[†,‡] Molamma P. Prabhakaran,*[,‡] Dariush Semnani,[†] Shahnaz Razavi,[§] Maedeh Zamani,[‡] and Seeram Ramakrishna[‡,⊥]

[†]Department of Textile Engineering, Isfahan University of Technology, Isfahan 84156-83111, Iran

[‡]Center for Nanofibers and Nanotechnology, E3-05-14, Nanoscience and Nanotechnology Initiative, Faculty of Engineering, National University of Singapore, 2 Engineering Drive 3, Singapore 117576

[§]Department of Anatomical Sciences and Molecular Biology, School of Medicine, Isfahan University of Medical Sciences, Isfahan 81744-176, Iran

[⊥]Department of Mechanical Engineering, Faculty of Engineering, National University of Singapore, 2 Engineering Drive 3, Singapore 117576

ABSTRACT: The ability of mature smooth muscle cells (SMCs) to modulate their phenotype in response to environmental cues is a critical issue related to vascular diseases. A tissue engineered vascular graft shall promote the contractile phenotype of vascular SMCs. To this aim, Tecophilic/gelatin (TP/gel) was electrospun at different weight ratios of TP/gelatin (100:0, 70:30, 50:50, 30:70), leading to differences in biochemical and mechanical properties of the nanofibers which in turn influenced the phenotype of SMCs. Results indicated that both the substrate with higher ligand density and lower stiffness could enhance SMC contractility and reduce cell proliferation. However, observing the highest SMCs contractility on electrospun TP(70)/gel(30) among the composite scaffolds demonstrated stiffness as the most critical parameter. Due to conflicting effects of softness versus minor fraction of gelatin (reduced ligand density) within TP(70)/gel(30) fibers, a relatively high proliferation of SMCs was still observed on TP(70)/gel(30) scaffold. The surface of TP(70)/gel(30) scaffold was further modified through physical adsorption of gelatin molecules so as to increase the ligand density on its surface, whereby a functional vascular construct that promotes the contractile behavior of SMCs with low cell proliferation was developed.

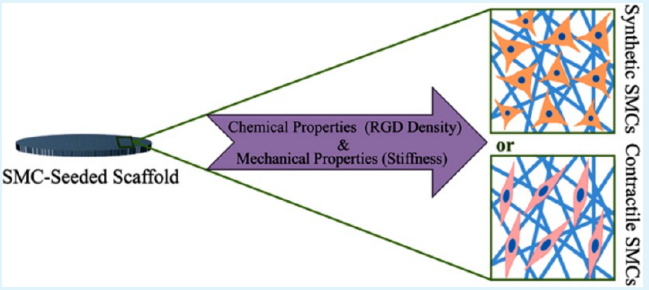

KEYWORDS: *contractile phenotype, electrospun scaffold, stiffness, ligand density*

INTRODUCTION

Many people suffer from cardiovascular disease, making it the leading cause of mortality worldwide. Plasticity of vascular smooth muscle cells (SMCs) plays a key role in regulating the vascular tone, remodeling, and disease development through phenotypic modulation/switching.[1−3] Vascular SMCs found in blood vessels, also known as the contractile SMCs, adopt an elongated and spindle-shaped morphology with an organized extracellular matrix (ECM) and express the contractile proteins, while they remain quiescent in proliferation and ECM metabolism.[1,2,4] Under pathological conditions of atherosclerosis and restenosis, vascular SMCs undergo transition to a synthetic (proliferative) phenotype often displaying a stellate shape, which is usually accompanied by an increase in ECM production with fewer contractile protein expression, and the cells become more mobile and proliferative.[1,2] SMCs with a synthetic phenotype migrate from the vascular wall into the lumen and rapidly proliferate, resulting in increased ECM deposition, neo-intimal formation, and arterial occlusion, known as neo-intimal hyperplasia or thickening which is considered as the precursor lesion for atherosclerosis in humans.[1,3,5]

Although the success rate of vascular prostheses with diameters larger than 6 mm has increased, intimal hyperplasia and ultimate atherosclerosis, restenosis, and occlusion account for the early failure of small caliber artificial vascular grafts.[6,7] In recent years, tissue engineering (TE) has received more attention as a promising alternative to overcome the limited availability of small diameter blood vessels. Complications similar to the aforementioned pathologies would happen due to the undesired outcome of implanting a vascular substitute containing cells in the proliferative state, and hence, an engineered vascular tissue should presumably be in a contractile or quiescent state for implantation.[8] Tissue engineered grafts have potential to control the phenotypic modulation of SMCs via managing the cell behavior over the surface of the scaffolds.

Received: December 10, 2013
Accepted: March 4, 2014
Published: March 4, 2014

 © 2014 American Chemical Society dx.doi.org/10.1021/am405673h | *ACS Appl. Mater. Interfaces* 2014, 6, 4089−4101

There is plenty of research that investigated the effect of biochemical and biomechanical factors on the phenotype of SMCs; however, few studies attempted to direct SMCs toward the contractile phenotype using TE methodologies. In order to investigate the simultaneous effects of surface chemistry (ligand density) and mechanical properties of the substrate (stiffness) on the phenotypic plasticity of SMCs, electrospun composite scaffolds of Tecophilic/gelatin (TP/gel) with various weight ratios of TP/gel were fabricated and explored in this study.

Tecophilic is a family of hydrophilic polyether-based thermoplastic aliphatic polyurethanes (PU). Polyurethanes are often used in blood-contacting devices due to their thrombo-resistance, elasticity, good compatibility with tissue and blood, and resistance to mechanical degradation.[9,10] However, due to the lack of surface cell recognition sites, pure PU is rarely applicable, and here, we prepared a blend of PU with gelatin, a biocompatible, biodegradable, and commercially available natural biopolymer derived from collagen.[11]

The main objective of this study was to construct an optimal scaffold with the appropriate degree of ligand density and stiffness which might promote the contractile behavior of SMCs, making it suitable for vascular regeneration. This report showed the ability of a well-designed tissue-engineered scaffold for developing a functional vascular construct, supporting the contractile mode of SMCs during tissue regeneration which might minimize the probability of vascular graft failure.

EXPERIMENTAL SECTION

Materials. Tecophilic (TP) with a trade name of (SP-80A-150) was a kind gift from Lubrizol. Gelatin (gel) type A (300 Bloom) from porcine skin, gelatin solution from bovine skin, 1,1,1,3,3,3-hexafluoro-2-propanol (HFP), and phosphate buffered saline (PBS) were all purchased from Sigma-Aldrich. Human aortic SMCs and smooth muscle cell medium (SMCM) were obtained from ScienCell Research Laboratories.

Scaffold Fabrication. TP and gelatin were blended at four different weight ratios of 100:0, 70:30, 50:50, and 30:70, in HFP to obtain a total concentration of 8% (w/v). After stirring for 24 h at room temperature, the polymer solutions were individually loaded into a 3 mL syringe capped with a 27 G blunted stainless steel needle. A high voltage electric field of 10 kV (Gamma High Voltage Research, FL) was applied to the polymer solution fed at a constant flow rate of 1 mL/h using a syringe pump (KD Scientific, Inc., MA) to draw fibers toward the 15 mm coverslips placed on the grounded flat collector wrapped in aluminum foil distanced at 12 cm from the needle tip. Electrospun scaffolds were transferred to a vacuum desiccator at ambient temperature for at least 48 h to eliminate residual solvents.

Morphological and Chemical Characterization. Electrospun scaffolds coated with gold (JEOL JFC-1600 Auto fine coater, Japan) were visualized using a field emission scanning electron microscope (SEM; FEI-QUANTA 200FQ12, Netherlands) at an accelerating voltage of 10 kV. The average diameter of the electrospun fibers was calculated from 100 random points chosen from at least three different respective SEM images using image analysis software (Image J, National Institutes of Health, USA).

Attenuated total reflectance Fourier transform infrared (ATR-FTIR) spectroscopic analysis was carried out at room temperature to characterize the surface functional groups of the electrospun scaffolds at a resolution of 4 cm^{-1} using an Avatar 360 spectrometer (Thermo Nicolet, Waltham, MA) over the range of 400−4000 cm^{-1}.

Stiffness Measurement. Scaffold stiffness was determined by a uniaxial tensile testing system (Instron 5943) with 50 N load capacity at an extension rate of 10 mm/min. The elastic modulus of the membranes prepared in rectangular shape of 30 mm length and 10 mm breadth was evaluated using an algorithm for Young's modulus determination provided by the Bluehill3 software over a strain from 0 to 5%. Mechanical tests were performed for at least 5 samples of both dried and hydrated (equilibrated with PBS overnight at 37 °C) samples. Stiffness was computed by multiplying the elastic modulus values with cross section area and dividing by gauge length (2 cm).

Cell Culture. SMCs were cultured at 37 °C in a humidified atmosphere of 5% CO_2 in a 150 cm^2 cell culture flask using the smooth muscle cell medium (SMCM), which included the basal medium with 2% fetal bovine serum (FBS), 1% of smooth muscle cell growth supplement (SMCGS), and 1% of penicillin/streptomycin solution (P/S). The culture medium was replaced every 3 days until the cells reached confluency.

Cell Seeding. Electrospun scaffolds were sterilized by UV radiation for 2 h, placed in a 24-well plate, washed 3 times with PBS, and subsequently prewetted by immersing in SMCM overnight to improve cell attachment efficacy.

Confluent cells in the cell culture flask were trypsinized, centrifuged at 1500 rpm for 5 min, counted using a hemocytometer, and seeded on the electrospun scaffolds and tissue culture polystyrene (TCP as the control) at a density of 10,000 cells per well.

Cytocompatibility and Proliferation Assay. Electrospun scaffolds of different ratios of TP/gel were assayed for cell viability using Live/Dead Viability/Cytotoxicity kit (Invitrogen) based on the simultaneous determination of live and dead cells with two probes of calcein AM and ethidium homodimer-1 (EthD-1) that measure the intracellular esterase activity and plasma membrane integrity, respectively. Briefly, 200 μL of 4 μM EthD-1 and 2 μM calcein AM solution prepared by mixing 2 mM EthD-1 and 4 mM calcein AM stock solutions in PBS (4:1:2000) was directly added to cell seeded scaffolds cultured for 7 days and incubated for 30 min at 37 °C. Samples were washed with PBS before imaging using a Leica DM IRB fluorescent microscope.

Cell proliferation on the scaffolds was evaluated by quantification of the mitochondrial metabolic activity using 3-(4,5-dimethylthiazol-2-yl)-5-(3-carboxymethoxyphenyl)-2-(4-sulfophenyl)-2H-tetrazolium (MTS) assay (CellTiter 96 AQueous One solution; Promega, Madison, WI). Briefly, after 1, 4, 7, and 10 days of cell culture, cell-seeded scaffolds were rinsed with PBS, incubated in 1 mL of serum free medium containing 20% of MTS reagent at 37 °C for 3 h. The mixture was aliquoted into a 96-well plate (100 μL/well), and absorbance of the obtained dye was read using a spectrophotometric plate reader (FLUOstar Optima, BMG Lab Technologies, Offenburg, Germany) at 490 nm. Sample with culture medium but without cells was set to determine the background absorbance to be subtracted. The intensity of the obtained color is directly proportional to the metabolic activity of the cell population.

Cell Morphology. Morphological assessment of SMCs seeded on the electrospun scaffolds was implemented by SEM analysis. To determine whether there is any change in cell morphology over time, evaluation was performed after desired time points of 4, 7, and 10 days. Briefly, after removing the medium from the culture wells, cell−scaffold constructs were washed with PBS, fixed with 3% glutaraldehyde for 3 h, rinsed with distilled water, and dehydrated using a graded series of ethanol solutions (50, 70, 90, and 100% v/v). Later, the samples were treated with hexamethyldisilazane (Sigma) and allowed to air-dry in a fumehood at room temperature. Completely dried specimens were sputter coated with gold and analyzed by SEM.

Phenotypic Markers Detection. Immunofluorescent staining after 5 days of culture was performed to observe the phenotype and organization of SMCs on the nanofibrous scaffolds. Briefly, the samples were rinsed with PBS, fixed with formalin at room temperature for 20 min, and permeabilized with 0.1% Triton-X100 for 3 min at room temperature. After washing the samples thrice with PBS, the nonspecific binding sites were blocked using 3% bovine serum albumin for 90 min at room temperature. The samples were then incubated with either fluorescein isothiocyanate (FITC)-conjugated mouse monoclonal anti-human alpha smooth muscle actin (α-SMA) antibody (Sigma) or mouse monoclonal anti-human smooth muscle myosin heavy chain (SM-MHC) antibody (Abcam) at a dilution of 1:100 for 2 h at room temperature. Cell−scaffold constructs were washed three times with PBS. This was followed by incubation with secondary antibody for samples incubated with

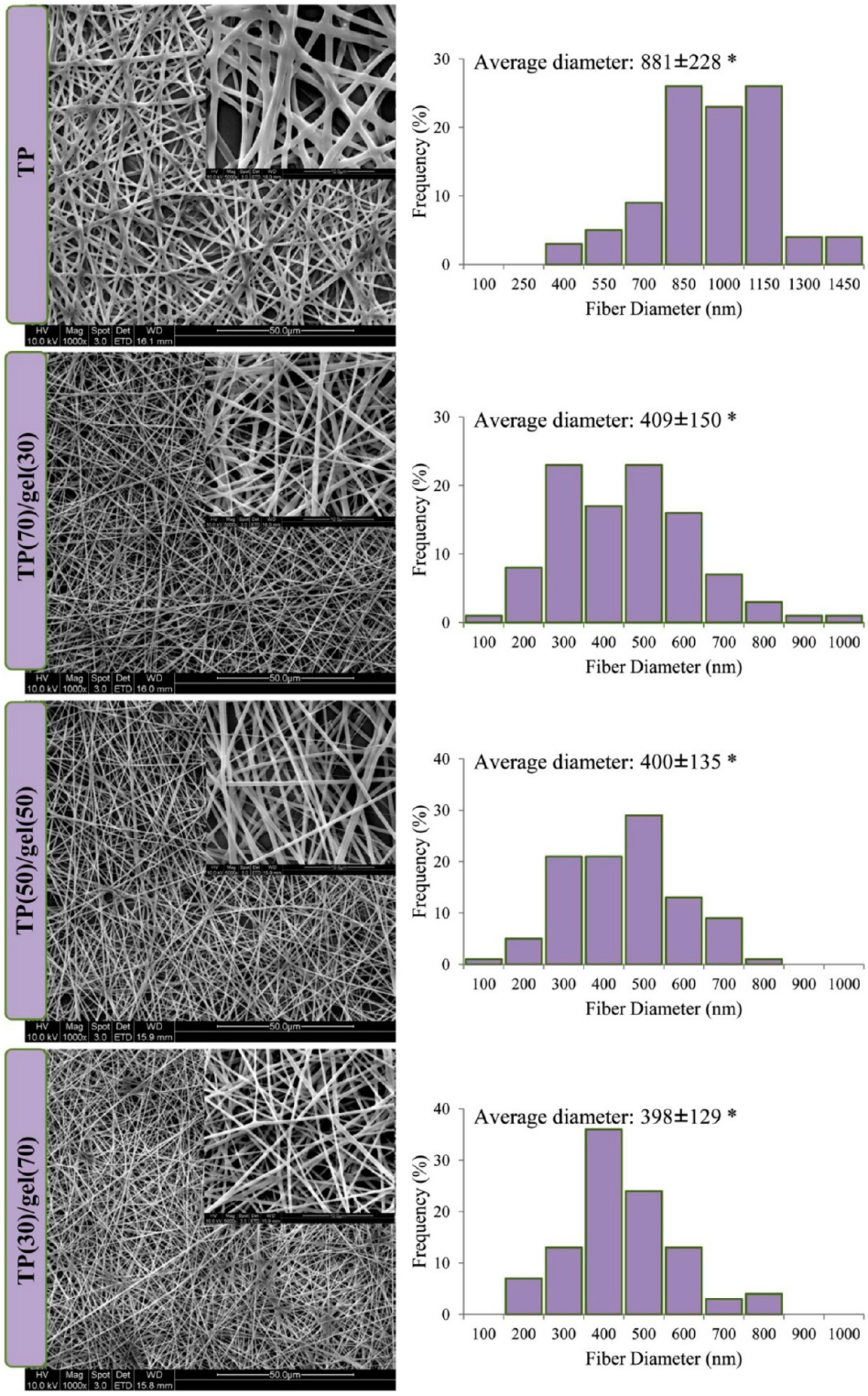

Figure 1. SEM micrographs and fiber diameter distribution of electrospun scaffolds; ∗ indicates significant differences compared to TP.

primary SM-MHC antibody, where a goat antimouse IgG Alexa Fluor-594 (Invitrogen) at a dilution of 1:400 for 90 min at room temperature was used. The cell nuclei were stained using a 1:500 dilution of 4′,6-diamidino-2-phenylindole, dihydrochloride (DAPI; Invitrogen). Further, the cell−scaffold constructs were washed, mounted over glass slides, and visualized under laser scanning confocal microscopy (Olympus, FluoView FV1000).

The nuclear alignment and shape index of DAPI-stained nuclei were measured for quantitative evaluation of overall cell alignment and elongation.[12] The alignment angle defined as the angle of the longest elliptic axis of individual nuclei with respect to the horizontal axis was determined from nuclei of 3 images of different regions of each sample using ImageJ. The histogram of alignment angles was plotted per sample, and average nuclear alignment within each sample was calculated and defined as the preferred nuclear orientation (PNO). The overall nuclear alignment per sample termed as alignment index (AI) was calculated from the average of three image measurements. Alignment of each image was calculated via dividing the number of

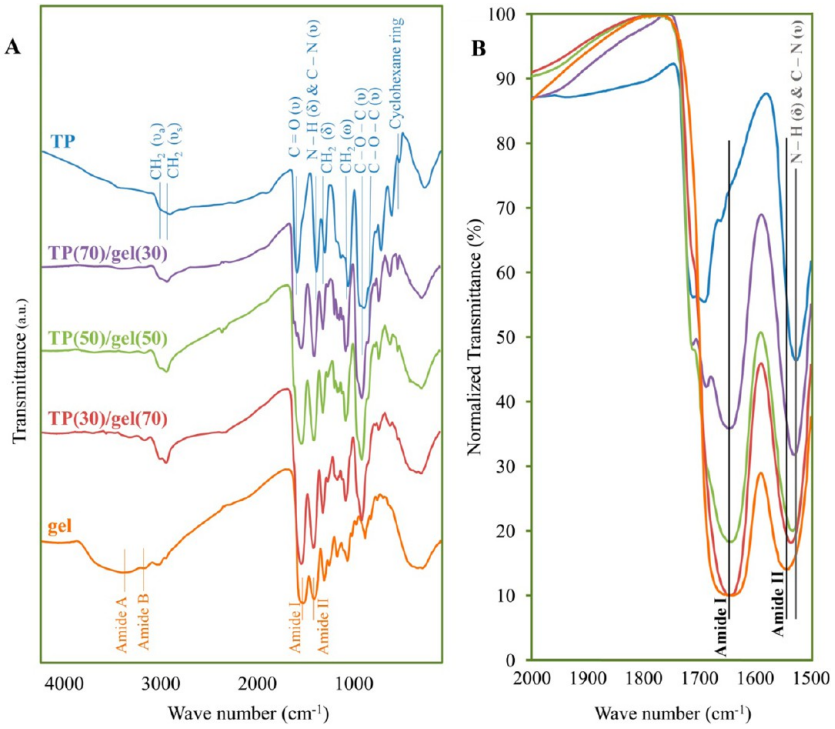

Figure 2. (A) FTIR spectra of electrospun scaffolds, (B) normalized spectra over the range of 1500−2000 cm^{-1}.

nuclei with an angle less or more than 10° with respect to preferred nuclear orientation by the total number of nuclei of the respective image. The projection area and perimeter of each nucleus within each image were measured using ImageJ software, and the nuclear shape index (NSI) was calculated from eq 1. Finally, the overall NSI was obtained by averaging the values of 60 points from three respective images. The NSI values ranged from 0 to 1, where values close to 0 and 1 are, respectively, referred to as elongated and circular morphology of cells.

$$\mathrm{NSI} = \frac{4\pi \cdot \mathrm{area}}{(\mathrm{perimeter})^2} \quad (1)$$

Quantification of Matrix Proteins Expression. Expression of two major components of vascular ECM, namely, elastin and collagen, was evaluated qualitatively and quantitatively using immunofluorescent staining at day 5 and Sircol Soluble Collagen Assay kit (Biocolor Ltd.) at day 10, respectively.

For immunofluorescent staining of synthesized elastin protein, expression studies were performed using rabbit polyclonal anti-Elastin antibody (Abcam) and goat antimouse IgG Alex Fluor-488 conjugate as the primary and secondary antibodies, respectively, similar to that described under section Phenotypic Markers Detection.

For collagen quantification, after removing the culture medium, samples were rinsed with PBS, weighed, and digested in 1 mL of pepsin solution (pepsin (Sigma) dissolved in 2.0 M acetic acid (Sigma), 0.2 mg/mL) at 4 °C overnight and reacted with Sircol Dye reagent following the manufacturer's protocol and the obtained color was measured by a microplate reader at 540 nm. Standard curves were also prepared during this study using pure collagen solution provided by the supplier and were used to calculate the average of collagen content from duplicate samples. Acellular samples under similar culture conditions of cell seeded scaffolds were also assayed to subtract the background absorbance.

Designing the Optimized Construct. The results of cell studies presenting the impact of ligand density and scaffold stiffness toward the behavior of SMCs directed us to design an optimized scaffold that might cause the highest contractility with the least proliferation of cells. The optimized composition of the scaffold, so chosen, was further modified through physical adsorption of gelatin solution on the surface of the scaffold. In short, the scaffolds were immersed in gelatin solution (diluted in SMCM to obtain 10 μg/well) overnight before cell seeding. Cell proliferation and morphology were investigated for these optimized scaffolds according to described protocols (cell viability and MTS assays along with SEM analysis) and compared with cell behavior on respective untreated scaffolds.

Statistical Analysis. All data presented are expressed as mean ± standard deviation (SD). Statistical analysis was carried out using one-way ANOVA combined with Tukey post hoc tests for multiple-comparison of different samples. A value of $p < 0.05$ was considered statistically significant.

RESULTS

Morphological and Chemical Characterization. SEM micrographs of beadless and uniform randomly oriented fibers, shown in Figure 1, revealed the nanoscaled structure of the electrospun TP/gel fibers with fiber diameters in the range of 409 ± 150, 400 ± 135, and 398 ± 129 nm for TP(70)/gel(30), TP(50)/gel(50), and TP(30)/gel(70) scaffolds, respectively, whereas the fiber diameter of the electrospun pure TP was estimated as 881 ± 228 nm. Our results demonstrated the significant reduction ($p < 0.05$) in fiber diameter by incorporation of gelatin with TP. However, no significant changes in fiber diameter were observed between the TP/gel scaffolds, even after varying the amounts of gelatin in the composite scaffolds.

The results of ATR-FTIR analysis carried out for identification of chemical functionality of the electrospun scaffolds are shown in Figure 2A. Regarding the spectroscopic analysis of electrospun thermoplastic TP, the asymmetric stretching (υ_a) of methylene group was observed at 2935 cm^{-1} while its symmetric stretching (υ_s) was detected at 2856 cm^{-1}. The band observed at 1703 cm^{-1} can be assigned to the urethane C═O stretching (υ), and at the same time, both urethane N—H bending (δ) and C—N stretching (υ) were visible at 1530 cm^{-1}.

Urethane N—H bending (δ) and C—N stretching were also observed at 1310 cm^{-1}. In addition, the band at 1310 cm^{-1} was responsible for in plane bending (β) of C—H. The FTIR spectra also showed the aliphatic CH_2 bending (δ) and CH_2 wagging (ω) at 1450 and 1250 cm^{-1}, respectively. Stretching (υ) of C—O—C bond in aliphatic ether of soft and hard segments of TP was observed at 1110 and 1080 cm^{-1}, respectively, and the peak at 780 cm^{-1} arose from the cyclohexane ring.[13−16]

In addition, typical bands such as N—H stretching (υ) and C—H stretching (υ) for amide A and amide B were found at 3310 and 3068 cm^{-1} for the spectra of gelatin and TP/gel nanofibers. The presence of common indicative bands of gelatin in biocomposite TP/gel scaffolds was revealed at 1650 and 1540 cm^{-1} which belong to the amide I and amide II peaks corresponding to the stretching (υ) vibrations of C═O bond in the backbone of protein and coupling of N—H in plane bending (β) and C—N stretching (υ) in the gelatin, respectively.[17,18] N—H deformation for amide III was also detected at 1200−1300 cm^{-1}. The specific peaks of TP and gelatin, respectively, at 1530 and 1540 cm^{-1}, were found to be merged for TP/gel scaffolds, as is visible from the normalized FTIR spectra shown in Figure 2B; thus, a more prominent and broader peak was observed at this region of spectra compared to sharp individual peaks observed for pure TP and pure gelatin.[19]

Stiffness Measurement. Figure 3 shows the stiffness of the electrospun scaffolds in both dry and hydrated (i.e., after 24 h of soaking in PBS at 37 °C) conditions. In general, it was observed that the stiffness of the scaffolds increased by increasing the gelatin content which can be attributed to higher intrinsic stiffness of gelatin rather than TP. Among the composite scaffolds, electrospun TP(70)/gel(30) scaffold displayed the lowest stiffness in dry and hydrated conditions. The stiffness of electrospun TP, TP(70)/gel(30), TP(50)/gel(50), and TP(30)/gel(70) scaffolds, respectively, dropped from 0.38 ± 0.10, 1.06 ± 0.21, 5.63 ± 0.51, and 12.70 ± 0.98 N/mm^2 in dry conditions to 0.33 ± 0.09, 0.37 ± 0.07, 0.91 ± 0.21, and 2.74 ± 0.79 N/mm^2 in hydrated conditions. The stiffness reduction upon hydration was significantly profound for electrospun TP(50)/gel(50) and TP(30)/gel(70) scaffolds. Scaffolds of all compositions exhibited lower stiffness upon hydration conditions, which can be attributed to an increase in fiber tortuosity under hydrated conditions,[20] leading to higher elasticity and lower stiffness values.[21,22] Moreover, for hydrophilic polymers like TP and gelatin used in this study, the absorbed water acts as a plasticizer and increased the mobility of the polymeric chains resulting in more flexibility and lower stiffness of the scaffolds upon hydration.[23] In addition, the stiffness loss was higher for scaffolds with higher gelatin content, which can be explained due to the higher degradation rate of gelatin.[24,25]

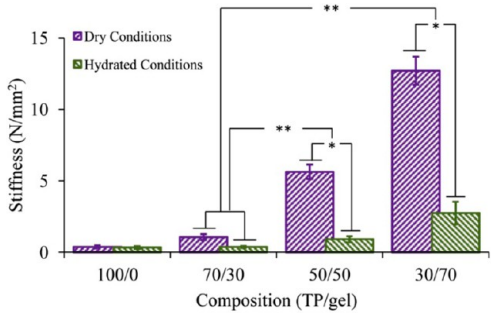

Figure 3. Stiffness values for electrospun TP, TP(70)/gel(30), TP(50)/gel(50), and TP(30)/gel(70) scaffolds under dry and hydrated conditions; * indicates significant differences between dry and hydrated conditions, and ** indicates significant differences from electrospun TP(70)/gel(30) scaffold.

Cytocompatibility and Proliferation Assay. The utility of the electrospun scaffolds for developing appropriate grafts for clinical transplantation was evaluated by cell viability and MTS assays, which estimate the effect of the scaffolds on the viability, growth, and metabolic behavior of SMCs. As shown in Figure 4A, cells continued to proliferate over time, confirming the ability of scaffolds to support cell growth, demonstrating their noncytotoxic behavior. Upon increasing the culture time, the statistical differences in cell proliferation between the samples appeared, such that the cell number on TP/gel scaffolds was significantly greater than on the electrospun TP scaffold but also lower compared to the cell growth on TCP. Mitochondrial metabolic activity of SMCs on electrospun TP(30)/gel(70) was significantly higher than that on other compositions ($p < 0.05$). Comparison of the cell proliferation on composite scaffolds showed the least potential of SMCs to grow on electrospun TP(50)/gel(50) scaffolds, even after 10 days of cell culture (Figure 4B).

Cell Morphology. Cell−scaffold interaction demonstrating the attachment, spreading, and shape of SMCs was observed using SEM on day 4, 7, and 10. The micrographs presented in Figure 5 reflect the status of cell attachment, spreading, and morphology. As shown in Figure 5 within 4 days of cell culture, less spindle shape was observed for SMCs on electrospun TP(70)/gel(30) while cells attached on electrospun TP(50)/gel(50) and TP(30)/gel(70) scaffolds as well as on TCP tended to be flat and pleomorphic. Over time, SMCs on electrospun TP(70)/gel(30) were self-oriented and elongated; thus, after 7 days of cell culture, they exhibited spindle like morphology and preserved this elongated spindle shaped morphology even after 10 days. However, no special organization was found for SMCs attached on other constructs after 7 days. In addition, SMCs on electrospun TP(50)/gel(50) were still flat, but due to a dense structure formed by the cells proliferated on TP(30)/gel(70) and TCP, the judgment of cell morphology on these constructs was difficult after 10 days of cell culture. However, a mild regularity appeared on the surface of the electrospun TP(30)/gel(70) which might be due to partial organization and elongation of SMCs over this scaffold after 10 days of cell culture.

Phenotypic Markers Detection. To determine the dependency of phenotype and organization of the SMCs on ligand density and stiffness of the produced electrospun scaffolds as synthetic ECM analogs, cells were stained with contractile marker proteins that are commonly used to define SMC phenotype including α-SMA and SM-MHC.[26] Representative images of α-SMA and SM-MHC of immunostained SMCs on various substrates generated via a confocal microscope after 5 days of culture time are displayed in Figure 6. Cells seeded on pure TP exhibited cell colony formation which can be attributed to high shrinkage capacity of pure TP due to its lower elasticity compared to other electrospun scaffolds of this study. Expression of α-SMA and SM-MHC by SMCs seeded on composite electrospun scaffolds, albeit not uniform among the various scaffolds, demonstrated their supportive feature for housing of SMCs. Figure 6 indicates the intense

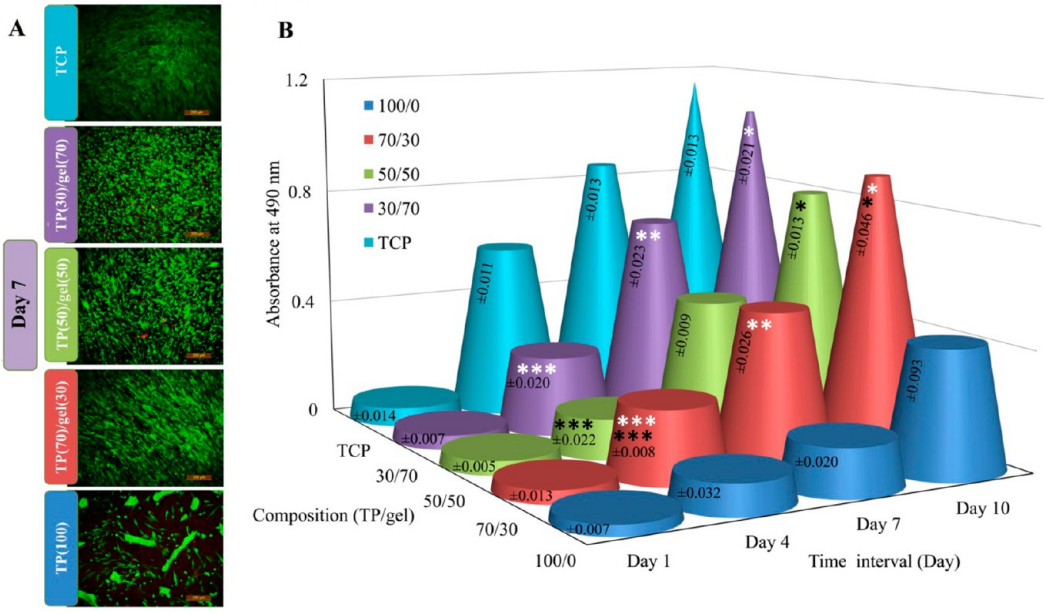

Figure 4. (A) Viability of SMCs on electrospun scaffolds using Live/Dead Viability/Cytotoxicity assay kit after 7 days of cell culture. (B) SMC proliferation on electrospun scaffolds and TCP; white ∗ indicates significant differences between electrospun TP(70)/gel(30) and TP(30)/gel(70) scaffolds while black ∗ indicates significant differences between electrospun TP(70)/gel(30) and TP(50)/gel(50) scaffolds. ±SD are shown within the chart.

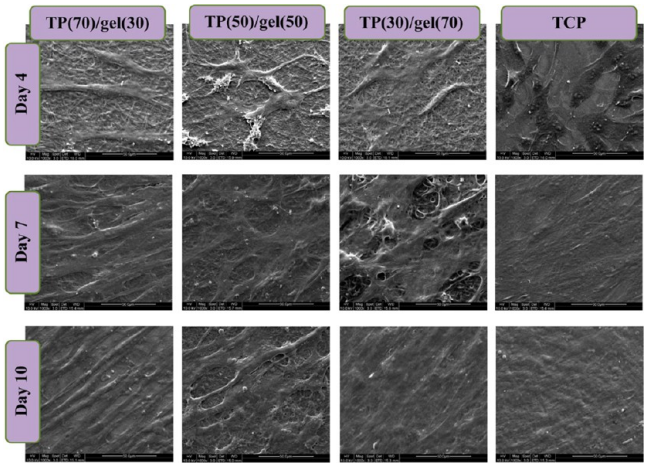

Figure 5. SEM images showing SMC−scaffold interactions on days 4, 7, and 10.

expression and organization of the contractile markers by SMCs on TP(70)/gel(30) with a well-elongated morphology corroborating the success of this construct to enhance SMC contractility. A minority of cells seeded on the electrospun TP(50)/gel(50) could express contractile markers. However, SMCs on the electrospun TP(30)/gel(70) were found to express α-SMA and SM-MHC markers better than on TP(50)/gel(50), albeit to a much lesser extent with a disordered organization compared to those on TP(70)/gel(30).

Scaffolds of different compositions induced different degrees of cell alignment. Histograms shown in Figure 7A,B revealed the random orientation of SMCs on electrospun TP(50)/gel(50) and TCP with alignment index of 8% ± 3% and 10% ± 1%, respectively. In contrast, a nearly oriented morphology (71% ± 4%) of SMCs was observed on electrospun TP(70)/gel(30) scaffolds. The alignment index of SMCs on electrospun TP(30)/gel(70) was estimated as 39% ± 6% which showed

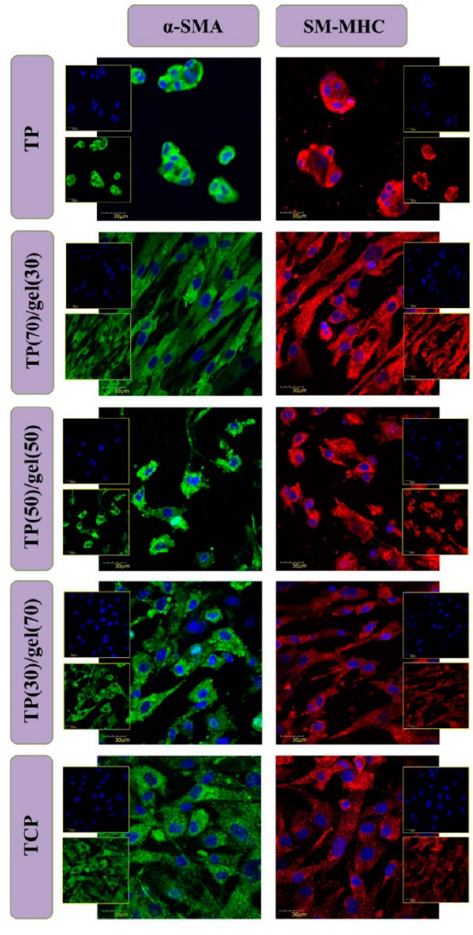

Figure 6. Immunocytochemical analysis on the expression of marker proteins of SMCs; α-smooth muscle actin (α-SMA) and smooth muscle myosin heavy chain (SM-MHC).

dx.doi.org/10.1021/am405673h | ACS Appl. Mater. Interfaces 2014, 6, 4089−4101

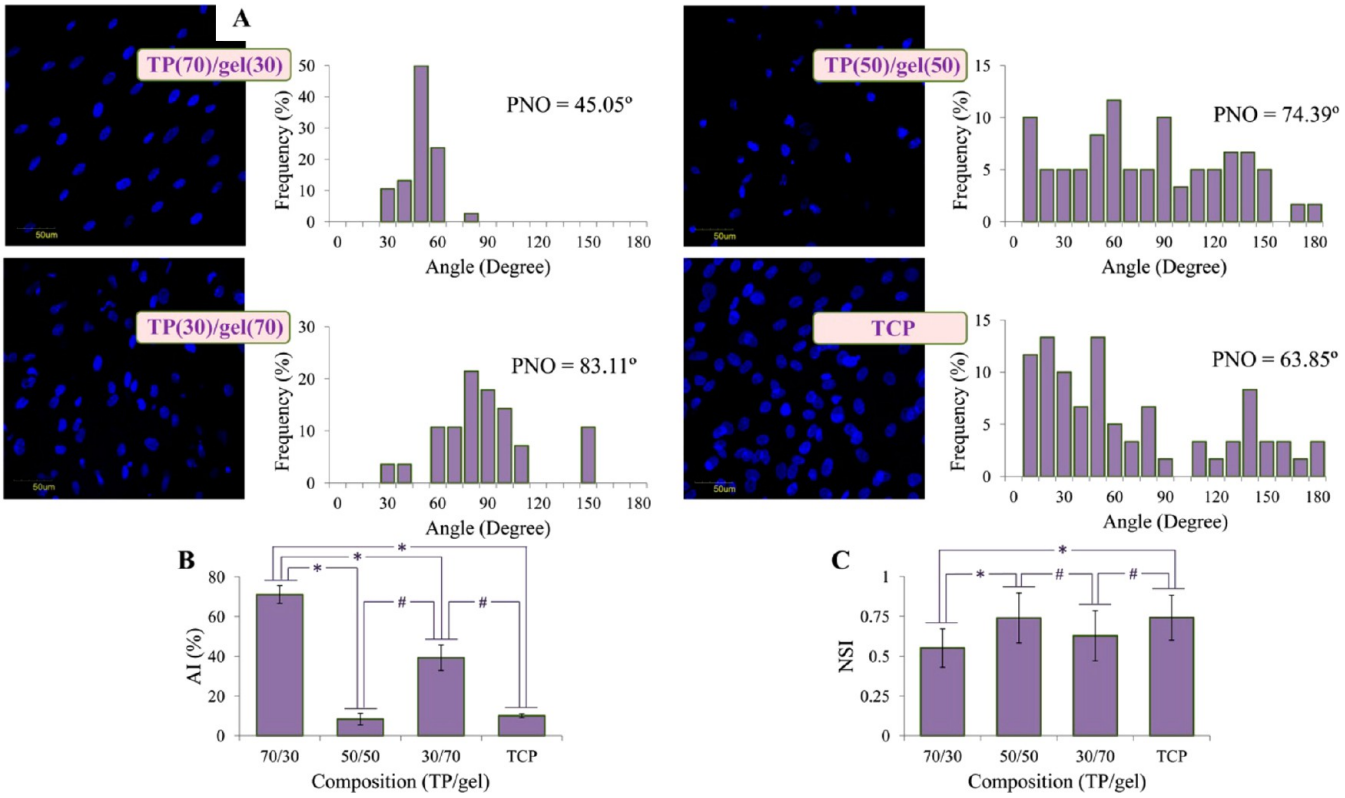

Figure 7. (A) Histograms showing the percentage of aligned cell nuclei in 10° increments and preferred nuclear orientation (PNO) with respect to DAPI staining of SMC-seeded structures. (B) Overall percentage of alignment index (AI) of cell nuclei (within 10° of PNO). (C) Overall nuclear shape index (NSI); ∗ indicates significant differences from electrospun TP(70)/gel(30) scaffold, and # indicates significant differences from electrospun TP(30)/gel(70) scaffold. (Calculating PNO, AI, and NSI for cells on pure TP was impossible due to their aggregation as the cell colonies.)

approximately a 5-fold increase in alignment of SMCs compared to cells on TP(50)/gel(50) scaffolds.

In addition, SMCs on the electrospun TP(70)/gel(30) exhibited significantly more elongated morphology with a NSI value of 0.55 ± 0.12 in comparison to on electrospun TP(50)/gel(50) and TCP (NSI = 0.73 ± 0.16 and 0.74 ± 0.14, respectively), while there was no meaningful differences in NSI of SMCs cultured on the electrospun TP(70)/gel(30) and TP(30)/gel(70) scaffolds (Figure 7C). A high value of AI as well as the reduced NSI value for SMCs cultured on TP(70)/gel(30) demonstrates the aligned orientation and elongated spindle-shape of SMCs confirming their contractile phenotype on electrospun TP(70)/gel(30) scaffolds.

Quantification of Matrix Proteins Expression. SMCs respond to the cellular environment through altering the expression of ECM proteins. As shown in Figure 8A–E, SMCs on all scaffolds biosynthesized the contractile ECM protein, namely, elastin.[27] However, up-regulation in the expression of elastin was sharply detected on the electrospun TP(70)/gel(30) scaffolds. On TP(70)/gel(30) scaffolds, elastin was found to be more organized around the cells, while a substantially lower degree of elastin expression was irregularly revealed on TP(50)/gel(50) and TP(30)/gel(70) scaffolds. Elastin production was, however, higher around cells on TP(30)/gel(70) compared to TP(50)/gel(50).

SMCs cultured on the various compositions of TP/gel exhibited different levels of collagen expression as observed in Figure 8F. After 10 days of culture, the collagen secretion by SMCs seeded on the electrospun TP(30)/gel(70) substrates was 74.64 ± 11.73 μg/g wet weight, which was significantly higher than collagen secretion on other scaffolds ($p < 0.05$) and still about 2-fold less compared to the amount of collagen deposits on TCP, corroborating the potential of TP/gel scaffolds in decreasing the synthetic characteristics of SMCs.

Among the composite scaffolds, consistent with results of cell proliferation, the minimum amount of collagen was expressed on TP(50)/gel(50) scaffolds with a value of 23.00 ± 6.71 μg/g wet weight. Collagen deposition on TP(70)/gel(30) was also estimated as 32.83 ± 18.75 μg/g wet weight.

Simultaneous Effects of Ligand Density and Stiffness of the Scaffolds. Briefly, the results of various cellular assays and analyses demonstrated a growing trend in cell proliferation, respectively, on TP(50)/gel(50),TP(70)/gel(30), and TP(30)/gel(70) scaffolds, while an upward trend in cell contractility was observed, respectively, on TP(50)/gel(50), TP(30)/gel(70), and TP(70)/gel(30). These complicated results arose from simultaneous changes in two effective parameters on cellular behavior including surface chemistry (ligand density) and mechanics (stiffness) by changing the polymeric composition. While increasing the ligand density improved the contractility of SMCs, increased stiffness regulated the SMCs toward a proliferative phenotype.[26,28] Thus, the lower stiffness of TP(70)/gel(30) scaffolds induced contractility of SMCs, whereas their lower ligand density directed the cells toward their synthetic characteristics. As a consequence of these conflicting effects, SMCs on TP(70)/gel(30) showed not only higher contractility compared to TP(50)/gel(50) and TC(30)/gel(70) scaffolds but also a higher rate of proliferation than on

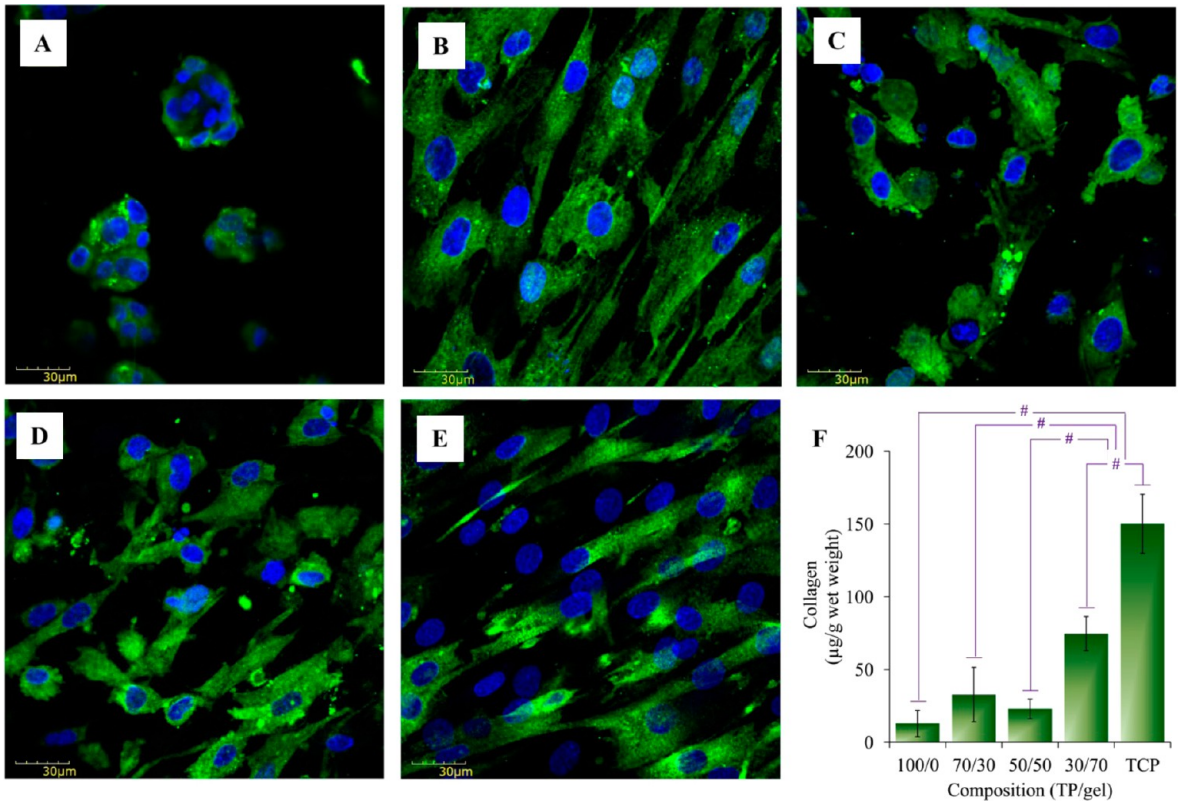

Figure 8. Matrix proteins expression; elastin deposited on electrospun (A) TP, (B) TP(70)/gel(30), (C) TP(50)/gel(50), (D) TP(30)/gel(70), and (E) TCP. (F) Deposited collagen; # indicates significant differences from the electrospun TP(30)/gel(70) scaffold.

TP(50)/gel(50) scaffolds. For SMCs seeded on TP(30)/gel(70) scaffolds, after a struggle between the highest stiffness of the scaffolds provoking the synthetic SMC phenotype and their highest ligand density promoting modulation toward the contractile phenotype, proliferation on these scaffolds was also higher than on TP(70)/gel(30) and TP(50)/gel(50) scaffolds, while SMCs gave the higher expression of the contractile markers compared to those on TP(50)/gel(50). All in all, in a competitive mode under these two conflicting effects, the scaffold stiffness displayed a greater impact in regulating the SMCs phenotype than ligand density. The results of comparative study on the simultaneous effects of ligand density and scaffold stiffness of electrospun TP/gel scaffolds are schematically shown in Figure 9. The resulting phenotype of SMCs on TP(50)/gel(50) with moderate stiffness and ligand density appeared to be neither proliferative nor contractile because both parameters canceled each other's effect out resulting in least cell proliferation and contractility.

Cell Behavior on Optimized Construct. In order to combine both these crucial parameters within a scaffold, such as to retain the cell contractile behavior along with a further reduction in proliferation, the scaffold with the least stiffness (TP(70)/gel(30)) was modified by physical adsorption of gelatin molecules. A comparative study was performed to evaluate the differences in behavior of SMCs on electrospun TP(70)/gel(30) scaffolds under two conditions (gelatin coated and noncoated surfaces). This study yet again confirmed the importance of ligand density in modulating the phenotypic behavior of SMCs while the scaffold stiffness remains constant.

As shown in Figure 10, cell proliferation decreased by 54%, 64%, 36%, and 20% on the TP(70)/gel(30)-coated samples after 1, 4, 7, and 10 days, respectively, compared to proliferation

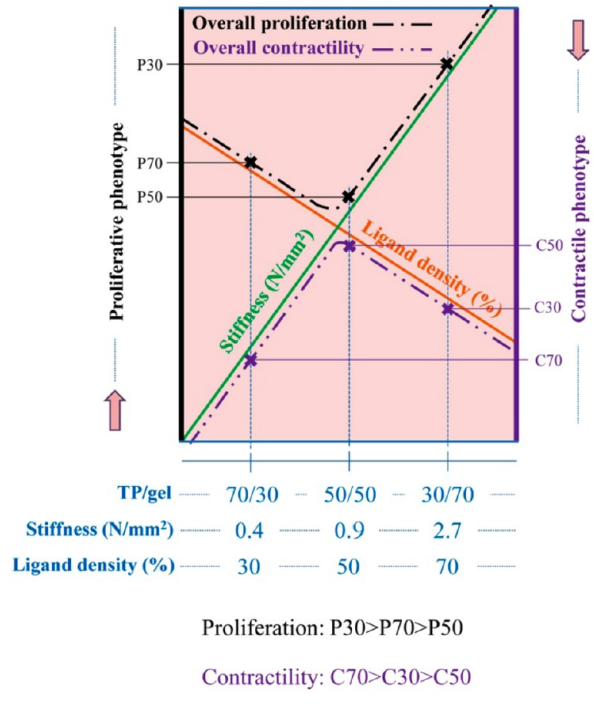

Figure 9. Schematic diagram showing how scaffold stiffness and ligand density affect the phenotypic regulation of SMCs. P70, P50, and P30 refer to cell proliferation on TP(70)/gel(30), TP(50)/gel(50), and TP(30)/gel(70) scaffolds, respectively. C70, C50, and C30 refer to cell contractility on TP(70)/gel(30), TP(50)/gel(50), and TP(30)/gel(70), respectively.

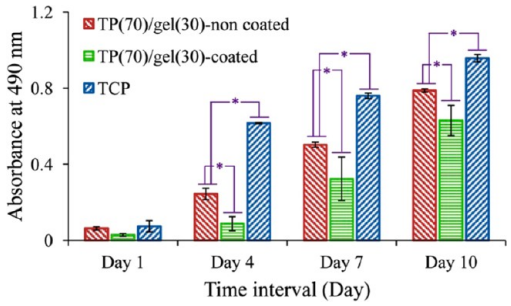

Figure 10. Proliferation of SMCs on electrospun TP(70)/gel(30)-noncoated and TP(70)/gel(30)-coated scaffolds; ∗ indicates significant differences from electrospun TP(70)/gel(30)-noncoated scaffold.

on noncoated scaffolds (Figure 10). This reduction in cell proliferation was accompanied by the preserved contractility phenotype of SMCs attached to the gelatin coated scaffold as seen in Figure 11A,B.

It is clear that, upon surface modification of TP(70)/gel(30) scaffolds with gelatin molecules, SMCs with spindle-shaped morphology are less proliferative compared to those on noncoated TP(70)/gel(30) scaffolds demonstrating the individual effect of RGD ligands to induce contractility of SMCs. In addition, combining the parameters of higher ligand density and lower stiffness could lead to development of a functional scaffold which supports the contractile behavior of SMCs that is required for vascular regeneration.

DISCUSSION

Physiological Changes in SMC Phenotype. SMCs are highly specialized cells which contribute significantly to the regulation of blood flow distribution, blood pressure, and blood vessel luminal diameter (vasodilation and vasoconstriction). SMCs in adult tissues proliferate scarcely under normal physiological conditions but respond to the local environment cues such as hypertension, vascular injury, and arteriosclerosis by major phenotypic adjustment from quiescent contractile to the active synthetic, migratory, or proliferative state. This phenotypic change as well as the failure to maintain the contractile phenotype results in migration and proliferation of SMCs and increased production of ECM proteins, which are the main reasons for various cardiovascular diseases such as the arteriosclerosis and restenosis.[29,30]

The unique ability of SMCs to change from contractile to proliferative (dedifferentiation) and turn into contractile from proliferative (redifferentiation) in response to the surrounding environment and growth factors[31] is an essentially missed factor that needs special consideration while fabricating scaffolds for vascular tissue regeneration. Many researchers have sought to identify the phenotypic modulation of SMCs as a function of innate genetic programs and environmental cues. In this regard, the effect of cell−cell interaction, ECM components, growth factors, local chemical conditions, and mechanical stimulations were discussed in various reviews.[2,8,26,30−32] In addition, regulatory mechanisms of phenotypic alterations of vascular SMCs have also been explored by many researchers.[33−36] An improved understanding of SMC phenotype with respect to the chemical, physical, and mechanical properties of the scaffolds is a novel approach, and it might be an advanced strategy of consideration during the development of functionally engineered constructs for vascular regeneration.

Effect of Scaffold Properties on Behavior of SMCs. The aim of this study was to control the phenotype of SMCs toward a contractile phenotype by reducing cell proliferation and increasing the expression of contractile marker proteins on electrospun TP/gel scaffolds of different compositions and

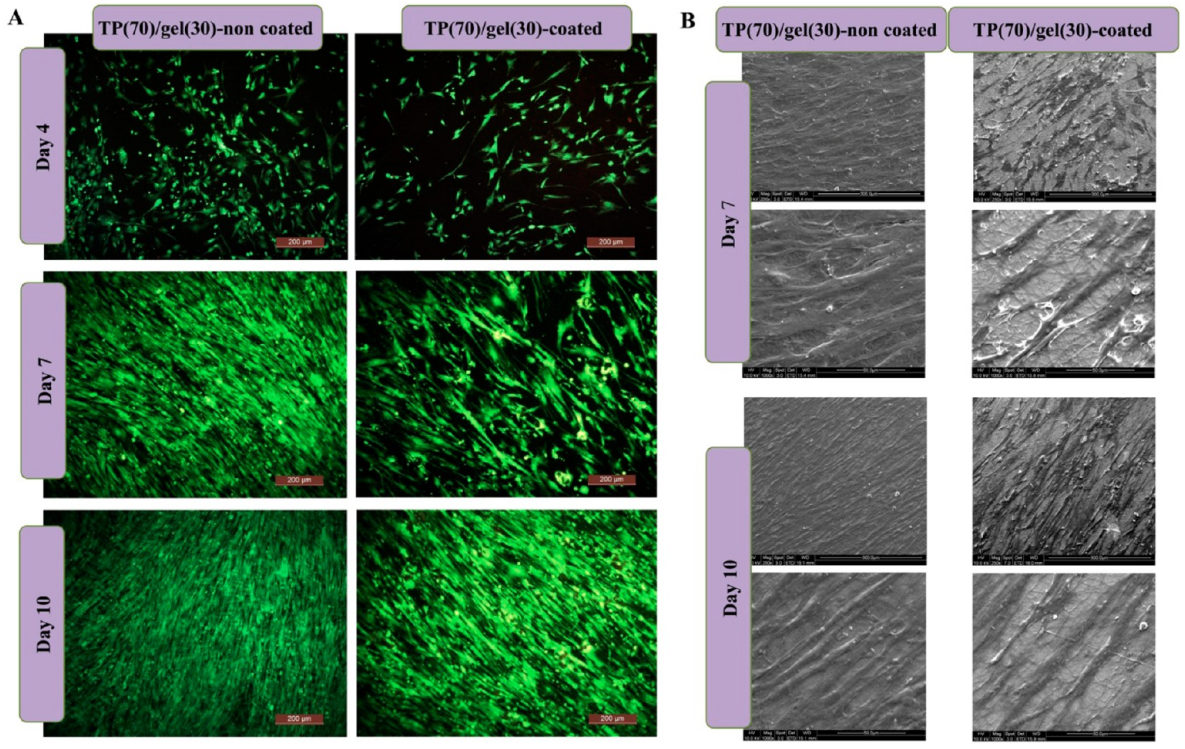

Figure 11. (A) Viability and (B) morphology of SMCs on electrospun TP(70)/gel(30)-noncoated and TP(70)/gel(30)-coated scaffolds.

dx.doi.org/10.1021/am405673h | ACS Appl. Mater. Interfaces 2014, 6, 4089−4101

stiffness, thus identifying the best optimized scaffold for vascular TE.

The scaffold-dependent variation in the SMC phenotype of engineered tissues could result from either the physical form of the applied materials (hydrogel versus solid structure) or the chemistry of the scaffold surfaces where the cell interaction takes place. Cells adhere to natural and synthetic polymeric scaffolds via different molecular cues, resulting in different patterns of gene expression.[37] Stiffness of the scaffold that serves as a biomimetic factor of the native ECM is a key mechanical attenuator of cell function during tissue formation. SMCs are cells with stiffness sensing ability, such that they detect mechanical resistivity of the extracellular environment and respond to it through the process of cell mechanotransduction. This ability is partly dependent on the actomyosin-generated contractility that is transmitted to the extracellular environment through transmembrane integrin receptors that, with a number of intracellular signaling pathways, creates the focal adhesion. In turn, cells respond to the stiffness of the substrate by altering their cytoskeletal organization, cell−substrate adhesion, and other processes regulating the cell behaviors.[5,38] To date, controlling the behavior of SMCs through the substrate stiffness was limited to hydrogels made of materials like polyacrylamide,[28,39−42] polydimethylsiloxane,[43] and poly(ethylene glycol).[44,45] Although fibrous structures are considered as the biomimetic environment of the native ECM, it was mainly the study by McDaniel et al. which reported the effect of stiffness of collagen fibrils toward vascular SMC phenotype.[46] Electrospun scaffolds, which are able to recapitulate both the structural and compositional features of vascular ECM with various elasticity, were used by Wingate et al. to direct mesenchymal stem cell differentiation to endothelial or smooth muscle cells.[47]

Despite the wide application of electrospun scaffolds in vascular TE,[4,48−50] there is a lack of information on the phenotypic response of SMCs to such fibrous constructs. In this study, the phenotypic plasticity of vascular SMCs on electrospun nanofibrous substrates of TP/gel with weight ratios of 100:0, 70:30, 50:50, and 30:70 were explored.

The behavior and regulation of cells depend on their response to topography, chemistry, and stiffness of the substrate on which they grow.[51] As shown in Figure 1, there is a drastic reduction in fiber diameter of composite scaffolds due to the addition of gelatin to TP, which can be attributed to the role of gelatin in decreasing the viscosity of the solution.[17] However, despite the decreasing trend in fiber diameter by increasing the gelatin content, no significant differences were observed in fiber diameter of the scaffolds prepared from various blending ratios of TP/gel. In addition, all scaffolds showed randomly oriented fibers. Therefore, in this study, there is minimal topographical variation of electrospun TP/gel scaffolds influencing the behavior of SMCs. On the other hand, the FTIR analysis (Figure 2) confirmed the presence of gelatin in composite TP/gel scaffolds, albeit the difference in ligand density of the scaffolds with different gelatin contents can influence the cellular response to the surface chemistry, affecting phenotypic modulation of SMCs. Cells adhere to the electrospun scaffolds via intrinsic cell adhesion molecules present in gelatin as well as the ECM proteins that are adsorbed on the polymer surfaces from the serum and growth supplement present in the culture medium.

Gelatin is a heterogeneous mixture of water-soluble proteins of high average molecular mass, similar to collagen extracted from porcine skin, and possesses many integrin binding sites (such as RGD) for cell adhesion.[52] It is considered to have nearly identical compositions and biological properties of collagen.[53] Distinct peaks observed at 1650 and 1540 cm^{-1} of the FTIR spectrum of gelatin correspond to the vibrations of amide I and amide II, which are representative of the RGD peptides. The "normalized FTIR spectra" (Figure 2B) illustrated pure gelatin as having the highest peak intensity of amide I and amide II. The intensity of the peaks gradually decreased with a decrease in gelatin content within the composite fibers. Additionally, comparing the spectra of the different TP/gel scaffolds of this study, it can be seen that a merged peak observed in the region of 1530−1540 cm^{-1} due to the merging of the specific peaks of TP and gelatin mainly shifted to a wavelength of 1530 cm^{-1}, for composite scaffolds with reduced gelatin content. Precisely, the merged peak was observed at 1531, 1533, and 1537 cm^{-1}, respectively, for TP(70)/gel(30), TP(50)/gel(50), and TP(30)/gel(70) scaffolds. These differences in FTIR spectra of composite scaffolds reflect an increase in RGD ligand density with an increase in the gelatin content within the composite scaffolds.

There are plenty of reports that describe the contradictory effects of various kinds of adhesion peptides toward phenotypic plasticity of SMCs. For example, it was reported by Hedin et al. that SMCs seeded on pure RGD peptide can dedifferentiate from contractile to proliferative,[54] while Beamish et al. showed that RGD-bearing poly(ethylene glycol) diacrylate (PEGDA) hydrogels support the contractile behavior of SMCs (α-actin and calponin expression).[55] Fibrillar collagen type I has also been shown to promote the contractile phenotype of SMCs, whereas monomeric collagen type I activates SMC proliferation.[26] Similarly, by means of the fibrous architecture of our electropsun scaffolds made from TP and gelatin, we anticipated that increasing the gelatin content persuades the cells to present a contractile phenotype.

The role of substrate stiffness in regulating the cellular response was elucidated here by measuring the stiffness of the substrata. The results of our previous studies showed that the ratio of the polymers is an important factor that affects the mechanical properties of a composite electrospun scaffold.[25] Therefore, we expected to obtain different values of stiffness for electrospun TP/gel scaffolds with different weight ratios. There are various methods utilized for determining the stiffness of the scaffolds such as uniaxial tension, while techniques like microindentation and AFM are exploited for local elasticity assessment.[51] Since both polymers used in the present study are hydrophilic materials, stiffness alteration due to water exposure was sought by performing the tensile tests of both dry and hydrated scaffolds. As can be seen in Figure 3, stiffness under both dry and hydrated conditions showed reduction upon decreasing the gelatin content within the scaffold, which also corroborates the softness of the electrospun scaffolds as TP(70)/gel(30) > TP(50)/gel(50) > TP(30)/gel(70). Various researchers correlated the increase in migration and proliferation of vascular SMCs with respect to substrate stiffness,[39−43,46] and such a claim suggests that the behavior of vascular SMCs gets altered owing to increased vessel stiffness during the development of vascular disease.[28]

Both scaffold composition and scaffold stiffness have had a major influence on the phenotype of SMCs, and these factors create a complicated situation with unpredictable behavior of SMCs, during this study. Increasing the TP content in the scaffold structure was accompanied with a reduction in ligand

density and decreased stiffness, which respectively direct the cells toward synthetic and contractile phenotypes. Investigating these conflicting effects can be helpful in identifying the dominant parameter that influences the behavior of SMCs.

As shown in Figures 4 and 5, compared to pure TP, SMCs seeded on the gelatin containing scaffolds (composite scaffolds) could recognize the cell binding sites provided by gelatin and readily attached to the fibrous matrix within 24 h of seeding. The proliferation behavior of cells on scaffolds was due to combined effects of chemical and mechanical features of the electrospun substrates, which revealed a substantially enhanced proliferation on electrospun TP(30)/gel(70) fibers over the time points indicating the dominant effect of scaffold stiffness rather than ligand density. As a result of SMCs response to two factors, namely, chemical and mechanical properties of TP(50)/gel(50), the proliferation rate was minimum on this scaffold in comparison to cell proliferation on TP(70)/gel(30), implying that the two aforementioned factors nearly nullified the effect of each other. Cells seeded on scaffolds of different compositions continued to proliferate over time with distinct morphologies (Figure 5). Cells on TP(70)/gel(30) showed spindle-like morphology and maintained this morphology over time. Additionally, the phenotypic behavior of the cells was examined by immunofluorescence staining of contractile markers of SMCs including α-SMA, SM-MHC, and elastin as seen in Figures 6, 7, and 8. Predominant expression of contractile proteins in an organized pattern was observed on low stiffness scaffold, namely, TP(70)/gel(30), and the organizational pattern is critical to discern the contractile state of seeded SMCs. While cells showed a rounded morphology with the weakest expression of contractile proteins on TP(50)/gel(50) scaffolds, low expression of contractile proteins was observed on TP(30)/gel(70) compared to that on TP(70)/gel(30) with a partly irregular organization.

In agreement with the findings of MTS assay, despite the contrary effects of ligand density and scaffold stiffness, the later parameter was demonstrated as the most effective factor in regulating the phenotype of SMCs. SMCs on electrospun TP(70)/gel(30) scaffolds exhibited more alignment and elongation compared to cells grown on other scaffolds. In addition, the least alignment index was observed for cells grown on electrospun TP(50)/gel(50) which confirms the least potential of this composition to enhance the contractile features of the cells seeded on it. Subsequent investigation on collagen expression over the constructs (Figure 8F) demonstrated that the collagen deposition was at least in part correlated with SMC proliferation and showed the highest level on TP(30)/gel(70) scaffold which can be considered as another confirmation of the dominant effect of scaffold stiffness toward the behavior of SMCs.

The lack of cell binding sites on pure TP along with its wrinkling and shrinkage effect caused the least attachment of cells on this scaffold and SMCs also formed irregularly localized shapes with a scattered distribution. Nevertheless, the amazing behavior of SMCs cultured on TP/gel in response to two parameters with incompatible effects induced us to believe that the scaffold stiffness can control the phenotype of SMCs to a much greater extent than ligand density. These inverse effects on proliferation and contractility of SMCs seeded on electrospun TP/gel scaffolds are schematically illustrated in Figure 9.

Although expression of the contractile markers closer to a contractile phenotype has been promising, partly high levels of cell proliferation and collagen deposition were still found on electrospun TP(70)/gel(30) due to lower gelatin content, envisioning the need for more attempts to reduce cell proliferation on this construct. Thus, we decided to combine both positive effects of the higher ligand density and the lower scaffold stiffness via increasing the ligand density over the electrospun TP(70)/gel(30) scaffold. Therefore, we immersed the electrospun TP(70)/gel(30) scaffolds in gelatin solution overnight before cell seeding to physically adsorb gelatin molecules on the surface of the scaffolds. The ability of this modified structure (TP(70)/gel(30)-coated) to preserve the contractility of SMCs in addition to its potential to decrease cell proliferation over the scaffold is shown in Figures 10 and 11.

The results of this study suggests that the effect of the engineered scaffolds toward the behavior of SMCs is a crucial factor of consideration, while aiming for a functional scaffold for vascular TE applications which unfortunately has received less attention until today. Since our qualitative examination of the phenotypic state of SMCs on electrospun scaffolds showed that the scaffold stiffness can serve as a dominant parameter to guide SMCs toward the contractile or synthetic states, additional studies using quantitative methods are suggested for future works.

CONCLUSION

Regulating the contractile phenotype of SMCs being crucial, the effect of different compositional ratios of TP/gel within an electropsun scaffold toward SMC plasticity was studied. Our results showed that higher ligand density and lower stiffness of a scaffold could encourage contractility of SMCs. While electrospun TP(30)/gel(70) provided the higher ligand density, the lowest stiffness was presented by TP(70)/gel(30) scaffold. With expression of contractile characteristics by SMCs on TP(70)/gel(30) scaffold, the stiffness of the scaffold was considered more crucial than ligand density in directing the contractile behavior of SMCs. Finally, to incorporate both the positive effects, an optimized structure was designed to dictate the highest contractility as well as low proliferation of SMCs by increasing the ligand density on the less stiffer scaffold of TP(70)/gel(30) through its surface modification. As expected, SMCs on TP(70)/gel(30)-coated scaffold maintained their contractility while having less proliferation than those on the noncoated TP(70)/gel(30) scaffold.

AUTHOR INFORMATION

Corresponding Author

*E-mail: nnimpp@nus.edu.sg.

Notes

The authors declare no competing financial interest.

ACKNOWLEDGMENTS

The authors gratefully acknowledge Lubrizol Corporation for kindly providing the "Tecophilic" polymer used in this research. This research was supported by NRF-Technion grant (R-398-001-065-592) and the Nanoscience and Nanotechnology Initiative, Faculty of Engineering, National University of Singapore, Singapore.

REFERENCES

(1) Han, Y.; Deng, J.; Guo, L.; Yan, C.; Liang, M.; Kang, J.; Liu, H.; Graham, A. M.; Li, S. CREG Promotes a Mature Smooth Muscle Cell

Phenotype and Reduces Neointimal Formation in Balloon-injured Rat Carotid Artery. *Cardiovasc. Res.* **2008**, *78*, 597−604.
(2) Chan-Park, M. B.; Shen, J. Y.; Cao, Y.; Xiong, Y.; Liu, Y.; Rayatpisheh, S.; Kang, G. C.-W.; Greisler, H. P. Biomimetic Control of Vascular Smooth Muscle Cell Morphology and Phenotype for Functional Tissue-Engineered Small-Diameter Blood Vessels. *J. Biomed. Mater. Res., A* **2009**, *88A*, 1104−1121.
(3) Thakar, R. G.; Cheng, Q.; Patel, S.; Chu, J.; Nasir, M.; Liepmann, D.; Komvopoulos, K.; Li, S. Cell-Shape Regulation of Smooth Muscle Cell Proliferation. *Biophys. J.* **2009**, *96*, 3423−3432.
(4) Blit, P. H.; Battiston, K. G.; Yang, M.; Paul Santerre, J.; Woodhouse, K. A. Electrospun Elastin-Like Polypeptide Enriched Polyurethanes and Their Interactions with Vascular Smooth Muscle Cells. *Acta Biomater.* **2012**, *8*, 2493−2503.
(5) Mason, B. N.; Califano, J. P.; Reinhart-King, C. A. Matrix Stiffness: A Regulator of Cellular Behavior and Tissue Formation. In *Engineering Biomaterials for Regenerative Medicine*; Bhatia, S. K., Ed.; Springer: New York, 2012; pp 19−37.
(6) Greenwald, S. E.; Berry, C. L. Improving Vascular Grafts: The Importance of Mechanical and Haemodynamic Properties. *J. Pathol.* **2000**, *190*, 292−299.
(7) Lee, S. J.; Yoo, J. J.; Lim, G. J.; Atala, A.; Stitzel, J. In Vitro Evaluation of Electrospun Nanofiber Scaffolds for Vascular Graft Application. *J. Biomed. Mater. Res., A* **2007**, *83A*, 999−1008.
(8) Stegemann, J. P.; Hong, H.; Nerem, R. M. Mechanical, Biochemical, and Extracellular Matrix Effects on Vascular Smooth Muscle Cell Phenotype. *J. Appl. Physiol.* **2005**, *98*, 2321−2327.
(9) Gunatillake, P. A.; Martin, D. J.; Meijs, G. F.; McCarthy, S. J.; Adhikari, R. Designing Biostable Polyurethane Elastomers for Biomedical Implants. *Aust. J. Chem.* **2003**, *56*, 545−557.
(10) Kampeerapappun, P. The Design, Characterization, and Application of Polyurethane Dressing Using the Electrospinning Process. Ph.D. Dissertation, The University of Akron, Akron, Ohio, 2008.
(11) Chong, E. J.; Phan, T. T.; Lim, I. J.; Zhang, Y. Z.; Bay, B. H.; Ramakrishna, S.; Lim, C. T. Evaluation of Electrospun PCL/Gelatin Nanofibrous Scaffold for Wound Healing and Layered Dermal Reconstitution. *Acta Biomater.* **2007**, *3*, 321−330.
(12) Aubin, H.; Nichol, J. W.; Hutson, C. B.; Bae, H.; Sieminski, A. L.; Cropek, D. M.; Akhyari, P.; Khademhosseini, A. Directed 3D Cell Alignment and Elongation in Microengineered Hydrogels. *Biomaterials* **2010**, *31*, 6941−6951.
(13) Srichatrapimuk, V. W.; Cooper, S. L. Infrared Thermal Analysis of Polyurethane Block Polymers. *J. Macromol. Sci. B* **1978**, *15*, 267−311.
(14) McCarthy, S. J.; Meijs, G. F.; Mitchell, N.; Gunatillake, P. A.; Heath, G.; Brandwood, A.; Schindhelm, K. In-vivo Degradation of Polyurethanes: Transmission-FTIR Microscopic Characterization of Polyurethanes Sectioned by Cryomicrotomy. *Biomaterials* **1997**, *18*, 1387−1409.
(15) Shanmugam, T.; Nasar, A. S. Novel Hyperbranched Poly(aryl ether urethane)s Using AB2-Type Blocked Isocyanate Monomers and Copolymerization with AB-Type Monomers. *Macromol. Chem. Phys.* **2008**, *209*, 651−665.
(16) Kim, S. E.; Heo, D. N.; Lee, J. B.; Kim, J. R.; Park, S. H.; Jeon, S. H.; Kwon, I. K. Electrospun Gelatin/Polyurethane Blended Nanofibers for Wound Healing. *Biomed. Mater.* **2009**, *4*, 044106.
(17) Meng, Z. X.; Wang, Y. S.; Ma, C.; Zheng, W.; Li, L.; Zheng, Y. F. Electrospinning of PLGA/Gelatin Randomly-Oriented and Aligned Nanofibers as Potential Scaffold in Tissue Engineering. *Mater. Sci. Eng., C* **2010**, *30*, 1204−1210.
(18) Ki, C. S.; Baek, D. H.; Gang, K. D.; Lee, K. H.; Um, I. C.; Park, Y. H. Characterization of Gelatin Nanofiber Prepared from Gelatin−Formic Acid Solution. *Polymer* **2005**, *46*, 5094−5102.
(19) Jia, L.; Prabhakaran, M.; Qin, X.; Kai, D.; Ramakrishna, S. Biocompatibility Evaluation of Protein-Incorporated Electrospun Polyurethane-Based Scaffolds with Smooth Muscle Cells for Vascular Tissue Engineering. *J. Mater. Sci.* **2013**, *48*, 5113−5124.
(20) Ebersole, G. C.; Paranjape, H.; Anderson, P. M.; Powell, H. M. Influence of Hydration on Fiber Geometry in Electrospun Scaffolds. *Acta Biomater.* **2012**, *8*, 4342−4348.
(21) Kao, P. H.; Lammers, S. R.; Hunter, K.; Stenmark, K. R.; Shandas, R.; Qi, H. J. Constitutive Modeling of Anisotropic Finite-Deformation Hyperelastic Behaviors of Soft Materials Reinforced by Tortuous Fibers. *Int. J. Struct. Changes Solid* **2010**, *2*, 19−29.
(22) Ohmura, J. Effects of Elastic Modulus on Single Fiber Uniaxial Deformation. Undergraduate Honors Thesis, The Ohio State University, Columbus, OH, 2011.
(23) Ping, Z. H.; Nguyen, Q. T.; Chen, S. M.; Zhou, J. Q.; Ding, Y. D. States of Water in Different Hydrophilic Polymers — DSC and FTIR Studies. *Polymer* **2001**, *42*, 8461−8467.
(24) Vatankhah, E.; Prabhakaran, M. P.; Jin, G.; Mobarakeh, L. G.; Ramakrishna, S. Development of Nanofibrous Cellulose Acetate/Gelatin Skin Substitutes for Variety Wound Treatment Applications. *J. Biomater. Appl.* **2014**, *28*, 909−921.
(25) Vatankhah, E.; Semnani, D.; Prabhakaran, M. P.; Tadayon, M.; Razavi, S.; Ramakrishna, S. Artificial Neural Network for Modeling the Elastic Modulus of Electrospun Polycaprolactone/Gelatin Scaffolds. *Acta Biomater.* **2014**, *10*, 709−721.
(26) Rensen, S. S. M.; Doevendans, P. A. F. M.; Eys, G. J. J. M. Regulation and Characteristics of Vascular Smooth Muscle Cell Phenotypic Diversity. *Neth. Heart J.* **2007**, *15*, 100−108.
(27) Wanjare, M.; Kuo, F.; Gerecht, S. Derivation and Maturation of Synthetic and Contractile Vascular Smooth Muscle Cells from Human Pluripotent Stem Cells. *Cardiovasc. Res.* **2013**, *97*, 321−330.
(28) Brown, X. Q.; Bartolak-Suki, E.; Williams, C.; Walker, M. L.; Weaver, V. M.; Wong, J. Y. Effect of Substrate Stiffness and PDGF on the Behavior of Vascular Smooth Muscle Cells: Implications for Atherosclerosis. *J. Cell Physiol.* **2010**, *225*, 115−122.
(29) Boettger, T.; Beetz, N.; Kostin, S.; Schneider, J.; Krüger M, M.; Hein, L.; Braun, T. Acquisition of the Contractile Phenotype by Murine Arterial Smooth Muscle Cells Depends on the Mir143/145 Gene Cluster. *J. Clin. Invest.* **2009**, *119*, 2634−2647.
(30) Beamish, J. A.; He, P.; Kottke-Marchant, K.; Marchant, R. E. Molecular Regulation of Contractile Smooth Muscle Cell Phenotype: Implications for Vascular Tissue Engineering. *Tissue Eng., Part B* **2010**, *16*, 467−491.
(31) Shinohara, S.; Shinohara, S.; Kihara, T.; Miyake, J. Regulation of Differentiated Phenotypes of Vascular Smooth Muscle Cells. In *Current basic and pathological approaches to the function of muscle cells and tissues - from molecules to humans*; Sugi, H., Ed.; InTech: Rijeka, Croatia, 2012; pp 331−344.
(32) Owens, G. K. Regulation of Differentiation of Vascular Smooth Muscle Cells. *Physiol. Rev.* **1995**, *75*, 487−517.
(33) Hayashi, K. i.; Saga, H.; Chimori, Y.; Kimura, K.; Yamanaka, Y.; Sobue, K. Differentiated Phenotype of Smooth Muscle Cells Depends on Signaling Pathways through Insulin-like Growth Factors and Phosphatidylinositol 3-Kinase. *J. Biol. Chem.* **1998**, *273*, 28860−28867.
(34) Hayashi, K. i.; Takahashi, M.; Kimura, K.; Nishida, W.; Saga, H.; Sobue, K. Changes in the Balance of Phosphoinositide 3-Kinase/Protein Kinase B (Akt) and the Mitogen-activated Protein Kinases (ERK/p38MAPK) Determine a Phenotype of Visceral and Vascular Smooth Muscle Cells. *J. Cell Biol.* **1999**, *145*, 727−740.
(35) Schauwienold, D.; Plum, C.; Helbing, T.; Voigt, P.; Bobbert, T.; Hoffmann, D.; Paul, M.; Reusch, H. P. ERK1/2-Dependent Contractile Protein Expression in Vascular Smooth Muscle Cells. *Hypertension* **2003**, *41*, 546−552.
(36) Fisher, S. A. Vascular Smooth Muscle Phenotypic Diversity and Function. *Physiol. Genomics* **2010**, *42A*, 169−187.
(37) Kim, B.-S.; Nikolovski, J.; Bonadio, J.; Smiley, E.; Mooney, D. J. Engineered Smooth Muscle Tissues: Regulating Cell Phenotype with the Scaffold. *Exp. Cell Res.* **1999**, *251*, 318−328.
(38) Discher, D. E.; Janmey, P.; Wang, Y.-l. Tissue Cells Feel and Respond to the Stiffness of Their Substrate. *Science* **2005**, *310*, 1139−1143.

(39) Wong, J. Y.; Velasco, A.; Rajagopalan, P.; Pham, Q. Directed Movement of Vascular Smooth Muscle Cells on Gradient-Compliant Hydrogels. *Langmuir* **2003**, *19*, 1908−1913.
(40) Engler, A.; Bacakova, L.; Newman, C.; Hategan, A.; Griffin, M.; Discher, D. Substrate Compliance versus Ligand Density in Cell on Gel Responses. *Biophys. J.* **2004**, *86*, 617−628.
(41) Peyton, S. R.; Putnam, A. J. Extracellular Matrix Rigidity Governs Smooth Muscle Cell Motility in a Biphasic Fashion. *J. Cell. Physiol.* **2005**, *204*, 198−209.
(42) Isenberg, B. C.; DiMilla, P. A.; Walker, M.; Kim, S.; Wong, J. Y. Vascular Smooth Muscle Cell Durotaxis Depends on Substrate Stiffness Gradient Strength. *Biophys. J.* **2009**, *97*, 1313−1322.
(43) Brown, X. Q.; Ookawa, K.; Wong, J. Y. Evaluation of Polydimethylsiloxane Scaffolds with Physiologically-Relevant Elastic Moduli: Interplay of Substrate Mechanics and Surface Chemistry Effects on Vascular Smooth Muscle Cell Response. *Biomaterials* **2005**, *26*, 3123−3129.
(44) Peyton, S. R.; Raub, C. B.; Keschrumrus, V. P.; Putnam, A. J. The Use of Poly(ethylene glycol) Hydrogels to Investigate the Impact of ECM Chemistry and Mechanics on Smooth Muscle Cells. *Biomaterials* **2006**, *27*, 4881−4893.
(45) Peyton, S. R.; Kim, P. D.; Ghajar, C. M.; Seliktar, D.; Putnam, A. J. The Effects of Matrix Stiffness and RhoA on the Phenotypic Plasticity of Smooth Muscle Cells in a 3-D Biosynthetic Hydrogel System. *Biomaterials* **2008**, *29*, 2597−2607.
(46) McDaniel, D. P.; Shaw, G. A.; Elliott, J. T.; Bhadriraju, K.; Meuse, C.; Chung, K.-H.; Plant, A. L. The Stiffness of Collagen Fibrils Influences Vascular Smooth Muscle Cell Phenotype. *Biophys. J.* **2007**, *92*, 1759−1769.
(47) Wingate, K.; Bonani, W.; Tan, Y.; Bryant, S. J.; Tan, W. Compressive Elasticity of Three-Dimensional Nanofiber Matrix Directs Mesenchymal Stem Cell Differentiation to Vascular Cells with Endothelial or Smooth Muscle Cell Markers. *Acta Biomater.* **2012**, *8*, 1440−1449.
(48) Vaz, C. M.; van Tuijl, S.; Bouten, C. V. C.; Baaijens, F. P. T. Design of Scaffolds for Blood Vessel Tissue Engineering Using a Multi-Layering Electrospinning Technique. *Acta Biomater.* **2005**, *1*, 575−582.
(49) Zhang, X.; Thomas, V.; Xu, Y.; Bellis, S. L.; Vohra, Y. K. An In Vitro Regenerated Functional Human Endothelium on a Nanofibrous Electrospun Scaffold. *Biomaterials* **2010**, *31*, 4376−4381.
(50) Wang, H.; Feng, Y.; Fang, Z.; Yuan, W.; Khan, M. Co-electrospun Blends of PU and PEG as Potential Biocompatible Scaffolds for Small-Diameter Vascular Tissue Engineering. *Mater. Sci. Eng., C* **2012**, *32*, 2306−2315.
(51) Wong, J. Y.; Leach, J. B.; Brown, X. Q. Balance of Chemistry, Topography, and Mechanics at the Cell−Biomaterial Interface: Issues and Challenges for Assessing the Role of Substrate Mechanics on Cell Response. *Surf. Sci.* **2004**, *570*, 119−133.
(52) Hajiali, H.; Shahgasempour, S.; Naimi-Jamal, M. R.; Peirovi, H. Electrospun PGA/Gelatin Nanofibrous Scaffolds and Their Potential Application in Vascular Tissue Engineering. *Int. J. Nanomed.* **2011**, *6*, 2133−2141.
(53) Huang, Z.-M.; Zhang, Y. Z.; Ramakrishna, S.; Lim, C. T. Electrospinning and Mechanical Characterization of Gelatin Nanofibers. *Polymer* **2004**, *45*, 5361−5368.
(54) Hedin, U.; Bottger, B. A.; Luthman, J.; Johansson, S.; Thyberg, J. A Substrate of the Cell-Attachment Sequence of Fibronectin (Arg-Gly-Asp-Ser) Is Sufficient to Promote Transition of Arterial Smooth Muscle Cells from a Contractile to a Synthetic Phenotype. *Dev. Biol.* **1989**, *133*, 489−501.
(55) Beamish, J. A.; Fu, A. Y.; Choi, A.-j.; Haq, N. A.; Kottke-Marchant, K.; Marchant, R. E. The Influence of RGD-Bearing Hydrogels on the Re-expression of Contractile Vascular Smooth Muscle Cell Phenotype. *Biomaterials* **2009**, *30*, 4127−4135.